

Reduction of switching time in pentalayer nanopillar device with different biasing configurations



D. Aravinthan^a, P. Sabareesan^b, M. Daniel^{a,c,*}

^a Centre for Nonlinear Dynamics, School of Physics, Bharathidasan University, Tiruchirappalli, 620024, Tamilnadu, India

^b Centre for Nonlinear Science and Engineering, School of Electrical and Electronics Engineering, SASTRA University, Thanjavur, 613401, Tamilnadu, India

^c SNS Institutions, Coimbatore, 641049, Tamilnadu, India

ARTICLE INFO

Article history:

Received 7 May 2016

Received in revised form

5 August 2016

Accepted 8 August 2016

Available online 10 August 2016

Keywords:

Ultrafast magnetization dynamics

Magnetization switching

Spin transfer torque

Nanopillar

Switching time

ABSTRACT

The spin transfer torque assisted magnetization switching in a pentalayer nanopillar device is theoretically studied for different biasing configurations. The magnetization switching time is calculated for three different configurations (standard(no biasing), pinned layer biasing and free layer biasing), by numerically solving the governing dynamical Landau–Lifshitz–Gilbert–Slonczewski (LLGS) equation. The corresponding switching time for an applied current density of $3 \times 10^{11} \text{ Am}^{-2}$ is about 0.296 ns, 0.195 ns, and 0.108 ns respectively. Pinned layer biasing and free layer biasing increase the magnetization switching speed significantly. Reduction of switching time in the pinned layer biasing is due to the enhancement of spin transfer torque, whereas in the free layer biasing it is due to an additional magnetic torque which arises due to an applied magnetic field. The fastest magnetization switching is achieved for the free layer biasing configuration.

© 2016 Elsevier B.V. All rights reserved.

1. Introduction

Magnetization switching using the “Spin transfer torque” proposed by Slonczewski [1] and Berger [2], have recently attracted much interest due to its potential application in read/write heads [3], microwave frequency generators [4] and spin transfer torque random access memories (STTRAM) [5]. For STTRAM applications nanopillar must have small cell size ($4F^2$), fast access time (less than 10 ns), high endurance (10^{16}) and long retention time [6]. The basic element used in the STTRAM is a trilayer nanopillar which consists of two ferromagnetic layers separated by a non-magnetic metal layer. Out of the two ferromagnetic layers, first layer magnetization is fixed/pinned during the fabrication process with the help of anti-ferromagnet and it is called as pinned layer. The magnetization of another layer can be switched between two states either parallel or anti-parallel with respect to the pinned layer and it is called as free layer. Current passes through the pinned layer becomes spin polarized. The polarized current entered into the free layer via non-magnetic spacer layer produces a spin transfer torque due to the exchange interaction between the spins of conductive electrons and local magnetization [7]. As a response to spin transfer torque, the free layer magnetization

begins to process, turning like a spinning-top about its easy axis. If the applied current is below a critical value, the magnetization relaxes back to its easy axis [8]. If the applied current is just above the critical, the magnetization follows many cycles of precession until its direction is reversed. When the applied current is well above the critical, the magnetization quickly reaches its reversed state [9]. The reduction of critical current density required to initiate the magnetization switching and increase the speed of magnetization switching are the important issues in STTRAM applications [10].

In order to increase the spin transfer torque efficiency and the switching speed, Fuchs et al. [11] introduced a pentalayer structure by adding a spacer and ferromagnetic pinned layer above the free layer in the trilayer structure based on the proposal from Berger [12], and showed that spin torque efficiency is increased in the case of pinned layers in the pentalayer structure are anti-aligned. The spin transfer torque efficiency enhancement in the pentalayer nanopillar reduces the critical current density very much [13]. In 2007, Devolder et al [14] introduced a biasing in the trilayer structure and comparing the benefits of pinned layer and free layer biasing, and showed that magnetization switching speed is enhanced by biasing. Based on the above two studies, in the present work, we study the spin transfer torque switching in pentalayer nanopillar structure (pinned 1/spacer 1/free/spacer 2/pinned 2) for various biasing configurations. In the pentalayer nanopillar, second pinned layer magnetization is aligned anti-parallel to the first pinned layer magnetization and free layer magnetization is

* Corresponding author at: Centre for Nonlinear Dynamics, School of Physics, Bharathidasan University, Tiruchirappalli 620024, Tamilnadu, India.

E-mail address: danielcnld@gmail.com (M. Daniel).

initially aligned along its easy axis. First, we investigate the magnetization switching dynamics of the free layer for the above said configuration called as standard configuration(SC). Then, we study the switching process for pinned layer biasing and free layer biasing configurations. In the pinned layer biasing, either the magnetization of the first pinned layer or second pinned layer magnetization can be tilted with respect to the free layer easy axis. In the free layer biasing, the magnetization of the free layer is pulled away from the easy axis by an external magnetic field. Magnetization switching dynamics of the free layer is governed by the Landau–Lifshitz–Gilbert–Slonczewski (LLGS) equation and it is studied by numerically solving the LLGS equation.

The paper is organized as follows. In Section 2, description about the geometry of pentalayer nanopillar device and the construction of dynamical equation for magnetization switching process by LLGS equation are presented. Numerical studies of standard, pinned layer biasing and free layer biasing configurations and their results are discussed in Section 3. Finally, concluding remarks are made in Section 4.

2. Model and dynamical equation

The pentalayer nanopillar device considered for our study has three ferromagnetic layers (two pinned layers and one free layer) and two non-magnetic metal layers (spacer layers). A schematic diagram of the above device is shown in the Fig. 1. In the figure, the first pinned layer magnetization is aligned along the easy axis and second pinned layer magnetization is anti-aligned with respect to the first one and their magnetizations are fixed. In order to analyze the magnetoresistance behavior and read the magnetization status of the free layer, two different thickness of pinned layers (first (bottom) pinned layer with larger thickness than that of second (top) pinned layer) have been chosen and the procedure to read the magnetization status from the magnetoresistance study is discussed in detail elsewhere [15]. The free layer is sandwiched between two non-magnetic spacer layers. Magnetization of the free layer is free to move and it has in-plane magnetic anisotropy. The applied current is normal to the plane of device (along z -direction), and it becomes spin polarized while passing through the first pinned layer. The spin polarized current transferred through non-magnetic metal layer, produces a torque in free layer due to the change in the electron spin angular momentum and it switches the magnetization of the free layer. The non-participant and scattered electrons from the free layer is entered into the second pinned layer, but since its magnetization is in

anti-parallel direction, i.e. in high resistance configuration, the electrons are reflected back into the free layer and it produces an additional spin torque in the free layer [16]. This additional torque reduces the critical current density and also enhances the magnetization switching speed of the free layer. The magnetization switching process of the free layer in the pentalayer nanopillar device is governed by the LLGS equation and it can be written in dimensionless form as [17,18],

$$\frac{d\mathbf{m}}{d\tau} = -[\mathbf{m} \times \mathbf{h}_{\text{eff}}] - \alpha[\mathbf{m} \times (\mathbf{m} \times \mathbf{h}_{\text{eff}})] + a_j[\mathbf{m} \times (\mathbf{m} \times \mathbf{m}_{p1})] - a_j[\mathbf{m} \times (\mathbf{m} \times \mathbf{m}_{p2})]. \quad (1)$$

$$\mathbf{m} = (m^x, m^y, m^z), \quad \mathbf{m}^2 = m^{x2} + m^{y2} + m^{z2} = 1. \quad (2)$$

where α is the Gilbert damping parameter, $a_j = \frac{pJ}{\mu_0 e d M_s^2}$ is the spin transfer torque coefficient and its value is, positive when electrons flow from pinned layer to free layer and negative when electrons transfer from free layer to pinned layer [19]. p is the polarization factor, J is the current density applied from the source, \hbar is the reduced Planck's constant, μ_0 is the permeability of free space, e is the charge of an electron, d is the thickness of the free layer and M_s is the saturation magnetization of the free layer. \mathbf{m}_{p1} and \mathbf{m}_{p2} are unit magnetization vectors in first and second pinned layer respectively. To account the non-collinearity between the free layer easy axis and pinned layer magnetization, we shall write pinned layers magnetization as $\mathbf{m}_{p1} = \cos\theta_1 \mathbf{e}^x + \sin\theta_1 \mathbf{e}^y$ and $\mathbf{m}_{p2} = \cos(\pi + \theta_2) \mathbf{e}^x + \sin(\pi + \theta_2) \mathbf{e}^y$. Where θ_1 and θ_2 are the angle between the free layer easy axis and magnetization of the first and second pinned layer respectively. $\mathbf{m} = \frac{\mathbf{M}}{M_s}$ is the dimensionless magnetization of the free layer, and $\tau = \gamma M_s t$ is the dimensionless time, where γ is the gyromagnetic ratio of free electron. \mathbf{h}_{eff} is the effective field acting on the free layer and it can be written as,

$$\mathbf{h}_{\text{eff}} = \mathbf{h}_{ma} + \mathbf{h}_{shape} + \mathbf{h}_{ext}, \quad (3)$$

where \mathbf{h}_{ma} is the field contribution due to the magneto-crystalline anisotropy. Since the free layer has in-plane magneto-crystalline anisotropy along its easy axis (x -direction), the corresponding field can be written as $\mathbf{h}_{ma} = h_a m^x \mathbf{e}^x$. \mathbf{h}_{shape} is the term for the shape anisotropy caused by the demagnetizing field and it can be written as $\mathbf{h}_{shape} = -(N_x m^x \mathbf{e}^x + N_y m^y \mathbf{e}^y + N_z m^z \mathbf{e}^z)$. Since the free layer is in the xy -plane, $N_x = N_y = 0$ and $N_z = 1$. Therefore, the field due to shape anisotropy becomes, $\mathbf{h}_{shape} = -m^z \mathbf{e}^z$. \mathbf{h}_{ext} is the field contribution from the external applied field and it is applied

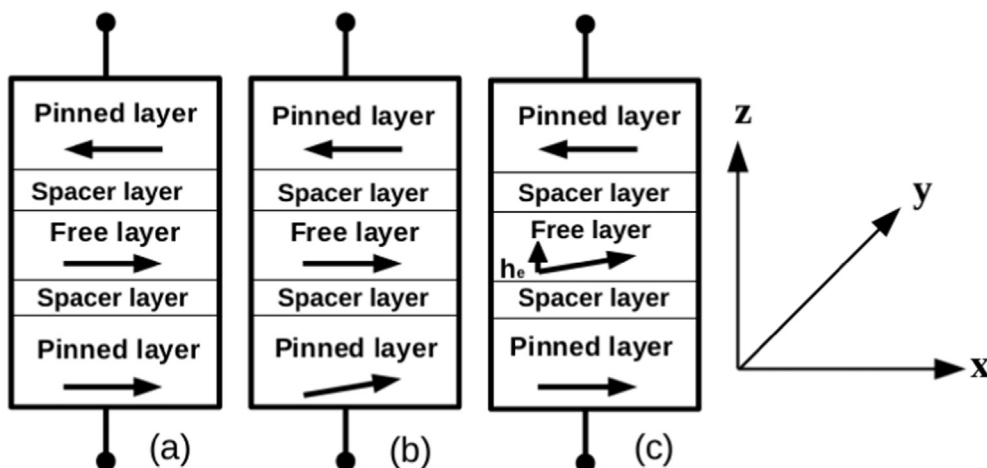


Fig. 1. Schematic sketch of the pentalayer nanopillar device. (a) Standard configuration (b) pinned layer biasing configuration (c) Free layer biasing configuration.

perpendicular to the easy axis of the free layer magnetization (y -direction) so $\mathbf{h}_{\text{ext}} = h_e \mathbf{e}^y$. From the above, the total effective field acting on the free layer can be rewritten as

$$\mathbf{h}_{\text{eff}} = h_a m^x \mathbf{e}^x + h_e \mathbf{e}^y - m^z \mathbf{e}^z. \quad (4)$$

By substituting the effective field found in Eq. (4) to Eq. (1), and the LLGS equation in component form can be written as,

$$\frac{dm^x}{d\tau} = (h_e + N_z m^y) m^z - \alpha [(h_e - h_a m^y) m^x m^y - (h_a + N_z) m^x m^z] + a_j [(\sin\theta_1 + \sin\theta_2) m^x m^y - (\cos\theta_1 + \cos\theta_2) (m^{y^2} + m^{z^2})] \quad (5)$$

$$\frac{dm^y}{d\tau} = -(h_a + N_z) m^x m^z + \alpha [(h_e - h_a m^y) m^{x^2} + (h_e + N_z m^y) m^{z^2}] - a_j [(\sin\theta_1 + \sin\theta_2) (m^{x^2} + m^{z^2}) - (\cos\theta_1 + \cos\theta_2) m^x m^y] \quad (6)$$

$$\frac{dm^z}{d\tau} = (h_a m^y - h_e) m^x - \alpha [(h_a + N_z) m^{x^2} m^z + (h_e + N_z m^y) m^y m^z] + a_j [(\sin\theta_1 + \sin\theta_2) m^y m^z + (\cos\theta_1 + \cos\theta_2) m^x m^z]. \quad (7)$$

By numerically solving the above set of first order differential equations, we can study the magnetization switching dynamics of the free layer in the pentalayer nanopillar and it is discussed in the forthcoming section.

3. Results and discussion

The set of first order LLGS equations (component form equations (Eq. (4))) is solved, by using the Runge–Kutta fourth order procedure, and the material parameters and constants used for the numerical simulations are given in the Table 1. Numerical results of the free layer magnetization switching dynamics for the standard configuration, pinned layer biasing configuration and free layer biasing configuration are discussed in the following sections.

3.1. Standard configuration

First the magnetization switching dynamics of the free layer for the standard configuration (SC) (Fig. 1(a)) is studied, by numerically solving the dimensionless first order LLGS equations given in Eqs. (4a)–(4c) using the Runge–Kutta fourth order procedure. After solving, the dimensionless time variable τ is converted into dimension time t by using the transformation $t = \frac{\tau}{\gamma M_s}$ and the results are plotted in Fig. 2. In which, Fig. 2(a) represents a plot of free layer magnetization against the switching time for an applied current density of $3 \times 10^{11} \text{ Am}^{-2}$. The applied current flowing to the pentalayer structure becomes spin polarized by transmission or reflection from the pinned layers. When the spin polarized current reaches the free layer, both interface of the free layer produces a

Table 1
Values of the various parameters used in the numerical simulations.

Parameter	Symbol	Value
Polarization factor	p	0.3
Gilbert damping parameter	α	0.003
Magneto-crystalline anisotropy of free layer	h_a	0.01
Saturation magnetization of free layer	M_s	$0.795 \times 10^6 \text{ Am}^{-1}$
Thickness of the free layer	d	$2.8 \times 10^{-9} \text{ m}$
Applied current density	J	$3.0 \times 10^{11} \text{ Am}^{-2}$
Applied magnetic field	h_e/h_a	0.4

spin transfer torques due to the exchange coupling between the spins of conductive electrons and local magnetization. As a response to spin transfer torques and damping torque, the free layer magnetization undergoes an elliptical precession around the easy axis and it reaches the hard axis at $m^y = -1$ (shown in the trajectory (1) of Fig. 2(b)). Demagnetizing field generated normal to the film plane due to the shape anisotropy, combines with spin transfer torques, push the magnetization from the hard axis to the reversed state by an another half precession cycle (shown in the trajectory (2) of Fig. 2(b)). We have chosen the value of the applied current density $J = 3.0 \times 10^{11} \text{ Am}^{-2}$ (well above the critical value $J_c = 0.669 \times 10^{11} \text{ Am}^{-2}$, critical current density is calculated based on the formula given in Ref. [20]) in order to suppress the oscillations in the magnetization switching. Moreover the strength of the spin transfer torques is very high compared to that of damping torque, hence the effect of damping on magnetization switching is subtle. So, there is no oscillations in the magnetization switching. The time taken to switch the magnetization from $\mathbf{m} = (1, 0, 0)$ to $\mathbf{m} = (-1, 0, 0)$ is called as switching time and its value is 0.296 ns for the standard configuration. The initial spin transfer torque (STT) in the standard configuration is very small for the applied current density, due to the small angle between the pinned layer magnetization and free layer easy axis [21]. It can be enhanced by means of either biasing the pinned layer or by biasing the free layer, and it is discussed in the forthcoming section.

3.2. Pinned layer biasing configuration

For pinned layer biasing (PLB), either the magnetization of first pinned layer can be tilted or second pinned layer magnetization can be tilted from the easy axis. We have studied PLB configuration by tilting the first pinned layer magnetization. To compare the pinned layer biasing and free layer biasing configurations, we chose the biasing parameter value of 0.4 in y -axis ($0.4\mathbf{e}^y$) leading to the same tilting position for all the cases. To change the biasing position of the pinned layer for the PLB configuration (shown in Fig. 1(b)), magnetization of the first pinned layer is tilted to 24° from the easy axis. i.e. $\mathbf{m}_{p1} = 0.9\mathbf{e}^x + 0.4\mathbf{e}^y$ and $\mathbf{m}_{p2} = -\mathbf{e}^x$. Solving the component form LLGS equation (Eq. (4)) for this case yield the results as plotted in Fig. 3. A plot of free layer magnetization against the switching time for an applied current density of $3 \times 10^{11} \text{ Am}^{-2}$ in the PLB configuration is shown in Fig. 3(a). STT develops due to the current passed through the biased pinned layer, is higher than that of non-biased pinned layer (i.e. standard configuration). The reason is that, the angle between the first pinned layer magnetization and free layer easy axis is high in the PLB case, and hence change in the spin angular momentum is also high. For the enhanced initial STT, magnetization of the free layer undergoes an elliptical precession around the easy axis by overcoming the damping torque and it reaches the hard axis at $m^y = +1$ (shown in the trajectory (1) of Fig. 3(b)), much faster than in SC. Then the torque produced due to the demagnetizing field combines with spin transfer torques pulls the magnetization from the hard axis to the easy axis in the reversed state by one more half precession cycle shown in the trajectory (2) of Fig. 3(b). We can see the switching speed difference from the spiraling path of the magnetization trajectory in y - z plane. Hence, the switching time for PLB configuration is reduced compared to that of standard configuration and its value is 0.195 ns.

3.3. Free layer biasing configuration

Finally, we study the magnetization switching dynamics for the free layer biasing configuration (FLB) (Fig. 1(c)). In which, the pinned layers are same in the standard configuration position (i.e. no biasing in the pinned layers) and the magnetization of the free

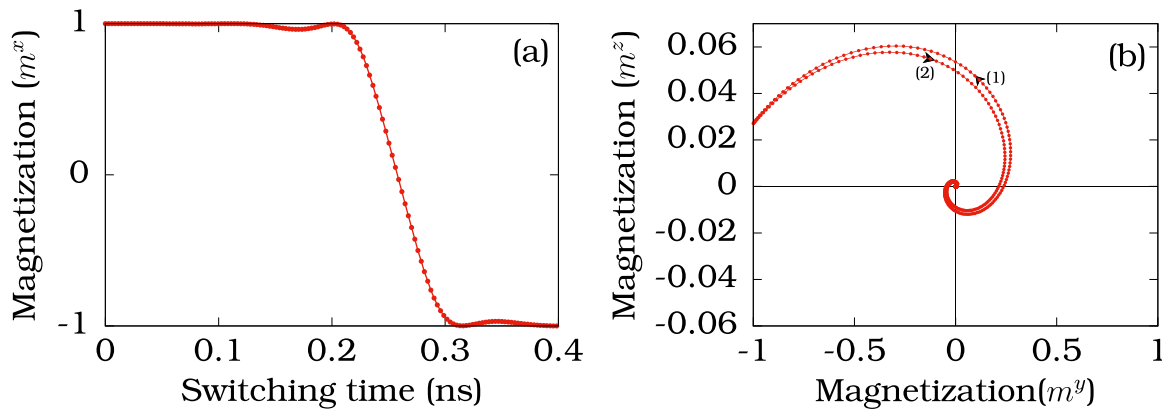


Fig. 2. (a). A plot of magnetization versus switching time (b). Magnetization trajectory in y - z plane for the standard configuration in the pentalayer nanopillar. In (b), (1) represents the first half (initial state ($m^y = 0, m^z = 0$) to out of plane) of the magnetization trajectory in y - z plane, (2) represents the second half (out of plane to final state ($m^y = 0, m^z = 0$)) of the magnetization trajectory in y - z plane.

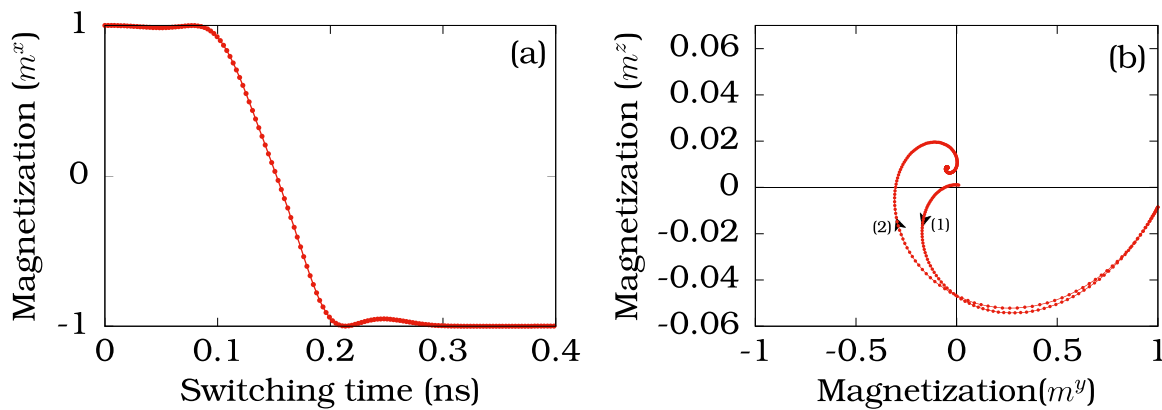


Fig. 3. (a). A plot of magnetization versus switching time (b). Magnetization trajectory in y - z plane for the pinned layer biasing configuration in the pentalayer nanopillar. In (b), (1) represents the first half (initial state ($m^y = 0, m^z = 0$) to out of plane) of the magnetization trajectory in y - z plane, (2) represents the second half (out of plane to final state ($m^y = 0, m^z = 0.01$)) of the magnetization trajectory in y - z plane.

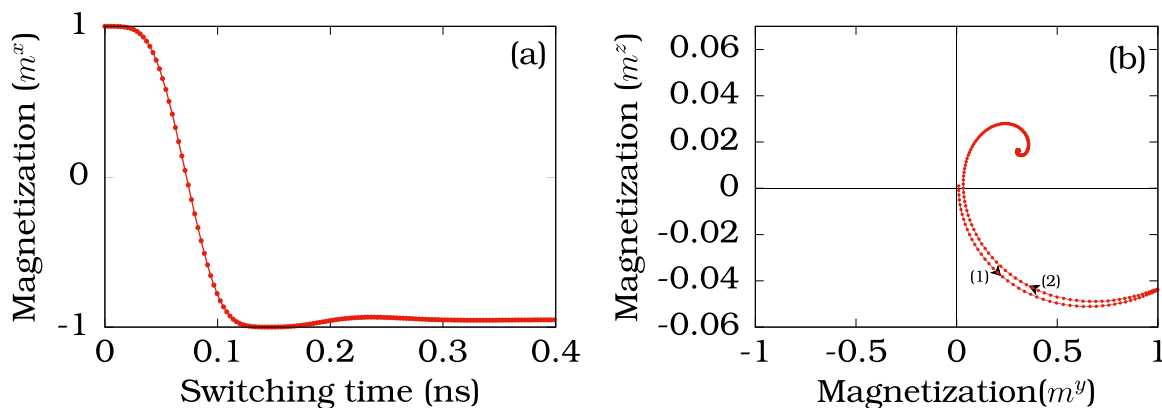


Fig. 4. (a). A plot of magnetization versus switching time (b). Magnetization trajectory in y - z plane for the free layer biasing configuration in the pentalayer nanopillar. In (b), (1) represents the first half (initial state ($m^y = 0, m^z = 0$) to out of plane) of the magnetization trajectory in y - z plane, (2) represents the second half (out of plane to final state ($m^y = 0.3, m^z = 0.01$)) of the magnetization trajectory in y - z plane.

layer is pulled away from the easy axis by an external magnetic field. Free layer magnetization is also biased to the same tilting parameter 0.4 ($h_e/h_a = 0.4\mathbf{e}^y$). Substituting the applied field value $h_e/h_a = 0.4\mathbf{e}^y$ in the component form LLGS equation (Eq. (4)) and solve the dynamical equation for an applied current density $3 \times 10^{11} \text{ Am}^{-2}$. The data obtained from numerical simulation is plotted in Fig. 4, and from Fig. 4(a), we can see that switching time for FLB configuration is further reduced to 0.108 ns . The reason behind this is that, magnetic field applied perpendicular to the free layer magnetization produces an additional magnetic torque and

this torque change the nature of the switching path in both ways. First, the magnetic torque combines with the damping torque and spin transfer torques move the free layer magnetization to the hard axis at $m^y = +1$ by a spiral contour from the easy axis shown in the trajectory (1) of Fig. 4(b). Then, the magnetic torque combines with the demagnetizing field and spin transfer torques pulls the magnetization from the hard axis to the easy axis in the reversed state ($m^y = 0.3, m^z = 0.01$) by another one spiral contour shown in the trajectory (2) of Fig. 4(b). Even though y and z component magnetization ($m^y = 0.3, m^z = 0.01$) is not reach zero,

switching is occurred in x component magnetization ($m^x = -1$). So, the spiraling path of the magnetization trajectory in y - z plane for FLB configuration is very short compared to that of SC and PLB configuration and hence the switching time is very low for this case. Therefore, the fastest switching is achieved for FLB configuration and it is in good agreement with the results obtained for the trilayer structure [14].

4. Conclusions

The spin transfer torque switching in pentalayer nanopillar for standard configuration, pinned layer biasing configuration and free layer biasing configuration are studied by numerically solving the governing dynamical LLGS equation. Their corresponding switching time is 0.296 ns, 0.195 ns and 0.108 ns respectively, for an applied current density $3 \times 10^{11} \text{ Am}^{-2}$. Even though the biasing in the pinned layer enhance the spin transfer torque acting on the free layer and reduces the switching time, the fastest magnetization switching is achieved for the free layer biasing configuration. In the free layer biasing, an additional magnetic torque is generated due to an applied magnetic field, which shorten the spiraling path of the magnetization trajectory and hence the switching time is reduced. The critical current density required to initiate the magnetization switching and the magnetization switching time can be reduced by making the pentalayer nanopillar with free layer biasing.

Acknowledgments

D.A acknowledges Department of Science and Technology

(DST) for the award of DST-INSPIRE Fellowship. P.S acknowledges DST for the award of SERB – Young Scientist project (SB/FTP/PS-061/2013).

References

- [1] J.C. Slonczewski, *J. Magn. Magn. Mater.* 159 (1996) L1.
- [2] L. Berger, *Phys. Rev. B* 54 (1996) 9353.
- [3] C. Chappert, A. Fert, F.N. Van Dau, *Nat. Mater.* 6 (2007) 813.
- [4] M. Carpentieri, F. Lattarulo, *IEEE Trans. Magn.* 49 (2013) 3151.
- [5] K. Wang, J. Alzate, P.K. Amiri, *J. Phys. D: Appl. Phys.* 46 (2013) 074003.
- [6] A. Makarov, V. Sverdlov, D. Osintsev, S. Selberherr, *Phys. Status Solidi RRL* 5 (2011) 420.
- [7] R.-X. Wang, P.-B. He, Z.-D. Li, A.-L. Pan, Q.-H. Liu, *J. Appl. Phys.* 109 (2011) 033905.
- [8] Z. Li, S. Zhang, *Phys. Rev. B* 68 (2003) 024404.
- [9] J. Sun, *Nature* 425 (2003) 359.
- [10] R. Sbiaa, S.Y.H. Lua, R. Law, H. Meng, R. Lye, H.K. Tan, *J. Appl. Phys.* 109 (2011) 07C707.
- [11] G.D. Fuchs, I.N. Krivorotov, P.M. Braganca, N.C. Emley, A.G.F. Garcia, D.C. Ralph, R.A. Buhrman, *Appl. Phys. Lett.* 86 (2005) 152509.
- [12] L. Berger, *J. Appl. Phys.* 93 (2003) 7693.
- [13] Y. Huai, M. Pakala, Z. Diao, Y. Ding, *Appl. Phys. Lett.* 87 (2005) 222510.
- [14] T. Devolder, C. Chappert, K. Ito, *Phys. Rev. B* 75 (2007) 224430.
- [15] B.S. Chun, C. Fowley, M. Abid, J.M.D. Coey, *J. Phys. D: Appl. Phys.* 43 (2010) 025002.
- [16] H. Meng, J. Wang, J.-P. Wang, *Appl. Phys. Lett.* 88 (2006) 082504.
- [17] D. Aravinthan, P. Sabareesan, M. Daniel, *AIP Adv.* 5 (2015) 077166.
- [18] A. Makarov, V. Sverdlov, D. Osintsev, S. Selberherr, *IEEE Trans. Magn.* 48 (2012) 1289.
- [19] M. Daniel, P. Sabareesan, *J. Magn. Magn. Mater.* 322 (2010) 675.
- [20] J.A. Katine, E.E. Fullerton, *J. Magn. Magn. Mater.* 320 (2008) 1217.
- [21] C.-Y. You, *Appl. Phys. Lett.* 100 (2012) 252413.